# Chapter 8

# Semiconductor Saturable Absorbers

Sofar we only considered artificial saturable absorbers, but there is of course the possibility to use real absorbers for modelocking. A prominent candidate for a saturable absorber is semiconductor material, which was pioneered by Islam, Knox and Keller [1][2][3] The great advantage of using semiconductor materials is that the wavelength range over which these absorbers operate can be chosen by material composition and bandstructure engineering, if semiconductor heterostructures are used (see Figure 8.1). Even though, the basic physics of carrier dynamics in these structures is to a large extent well understood [4], the actual development of semiconductor saturable absorbers for mode locking is still very much ongoing.

Figure 8.1: Energy Gap, corresponding wavelength and lattice constant for various compound semiconductors. The dashed lines indicate indirect transitions.
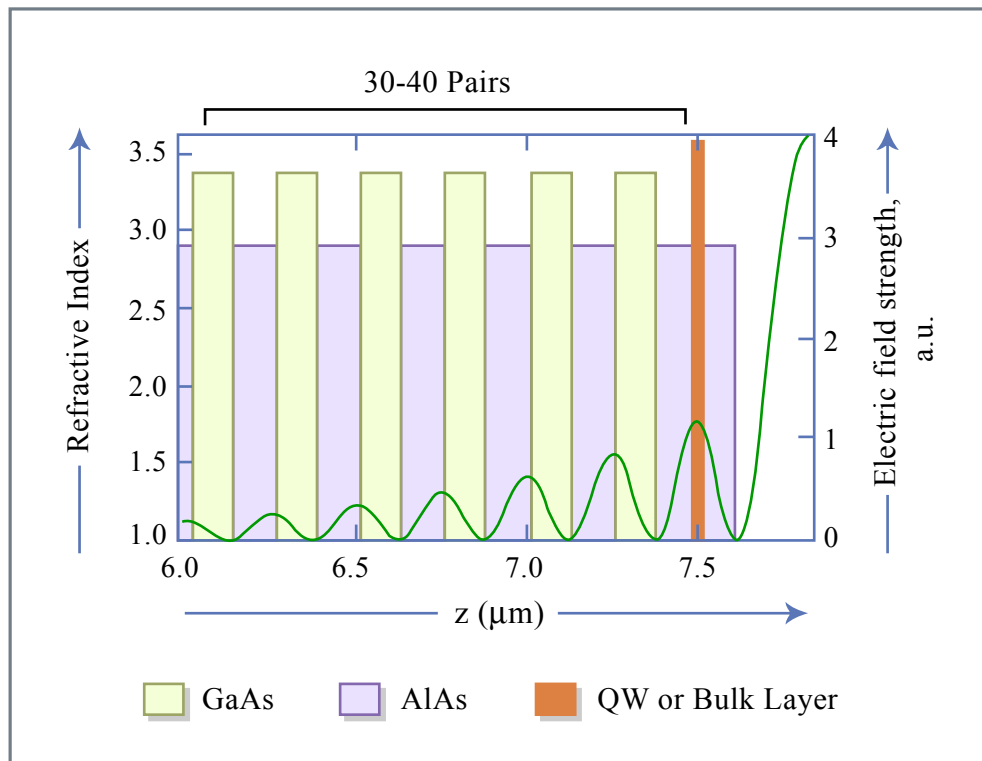


Figure 8.2: Typical semiconductor saturable absorber structure. A semiconductor heterostruture (here AlAs/GaAs) is grown on a GaAs-Wafer (20-40 pairs). The layer thicknesses are chosen to be quarter wave at the center wavelength at which the laser operates. This structures acts as quarter-wave Braggmirror. On top of the Bragg mirror a half-wave thick layer of the low index material (here AlAs) is grown, which has a field-maximum in its center. At the field maximum either a bulk layer of GaAlAs or a single-or multiple Quantum Well (MQW) structure is embedded, which acts as saturable absorber for the operating wavelength of the laser.

Figure by MIT OCW.

A typical semiconductor saturable absorber structure is shown in Figure 8.2. A semiconductor heterostruture (here AlAs/GaAs) is grown on a GaAs-Wafer (20-40 pairs). The layer thicknesses are chosen to be quarter wave at the center wavelength at which the laser operates. These structures act as quarter-wave Bragg mirror. On top of the Bragg mirror, a half-wave thick layer of the low index material (here AlAs) is grown, which has a field-maximum in its center. At the field maximum, either a bulk layer of a compound semiconductor or a single-or multiple Quantum Well (MQW) structure is embedded, which acts as a saturable absorber for the operating wavelength of the laser. The absorber mirror serves as one of the endmirrors in the laser (see Figure 8.3).
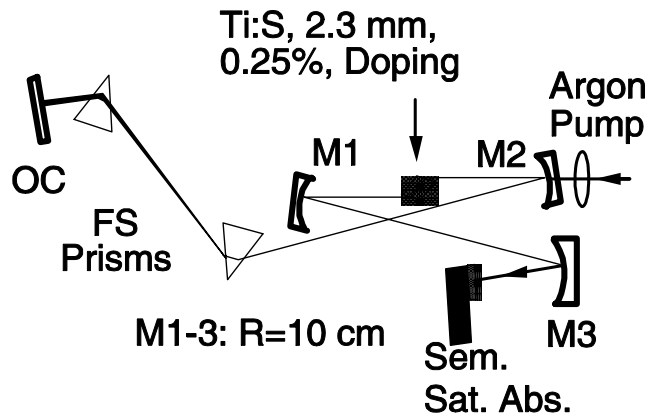
Figure 8.3: The semiconductor saturable absorber, mounted on a heat sink, is used as one of the cavity end mirrors. A curved mirror determines the spot-size of the laser beam on the saturable absorber and, therefore, scales the energy fluence on the absorber at a given intracavity energy.

# 8.1 Carrier Dynamics and Saturation Properties

There is a rich ultrafast carrier dynamics in these materials, which can be favorably exploited for saturable absorber design. The carrier dynamics in bulk semiconductors occurs on three major time scales (see Figure 8.4 [5]). When electron-hole pairs are generated, this excitation can be considered

as an equivalent two-level system if the interaction between the carriers is neglected, which is a very rough assumption.
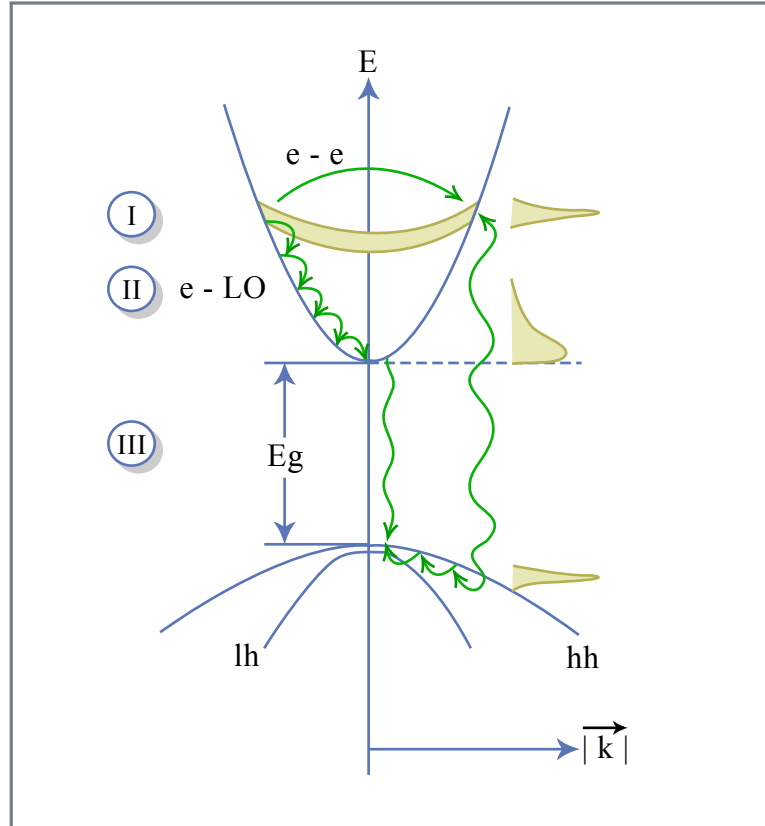


Figure 8.4: Carrier dynamics in a bulk semiconducotr material. Three time scales can be distinguished. I. Coherent carrier dynamics, which at room temperature may last between 10-50 fs depending on excitation density. II. Thermalization between the carriers due to carrier-carrier scattering and cooling to the lattice temperature by LO-Phonon emission. III. Carrier-trapping or recombination [5].

Figure by MIT OCW.

There is a coherent regime (I) with a duration of 10-50 fs depending on conditions and material. Then in phase (II), carrier-carrier scattering sets in and leads to destruction of coherence and thermalization of the electron and hole gas at a high temperature due to the excitation of the carriers high in the conduction or valence band. This usually happens on a 60 - 100 fs time scale. On a 300fs - 1ps time scale, the hot carrier gas interacts with the lattice mainly by emitting LO-phonons (37 meV in GaAs). The carrier gas cools down to lattice temperature. After the thermalization and cooling processes, the carriers are at the bottom of the conduction and valence band,

respectively. The carriers vanish (III) either by getting trapped in impurity states, which can happen on a 100 fs - 100 ps time scale, or recombine over recombination centers or by radiation on a nanosecond time-scale. Carrier-lifetimes in III-VI semiconductors can reach several tens of nanoseconds and in indirect semiconductors like silicon or germanium lifetimes can be in the millisecond range. The carrier lifetime can be engineered over a large range of values from 100 fs - 30ns, depending on the growth conditions and purity of the material. Special low-temperature growth that leads to the formation or trapping and recombination centers as well as ion-bombardment can result in very short lifetimes [9]. Figure 8.5 shows a typical pump probe response of a semiconductor saturable absorber when excited with a 100 fs long pulse. The typical bi-temporal behavior stems from the fast thermalization (spectral hole-burning)[7] and carrier cooling and the slow trapping and recombination processes.
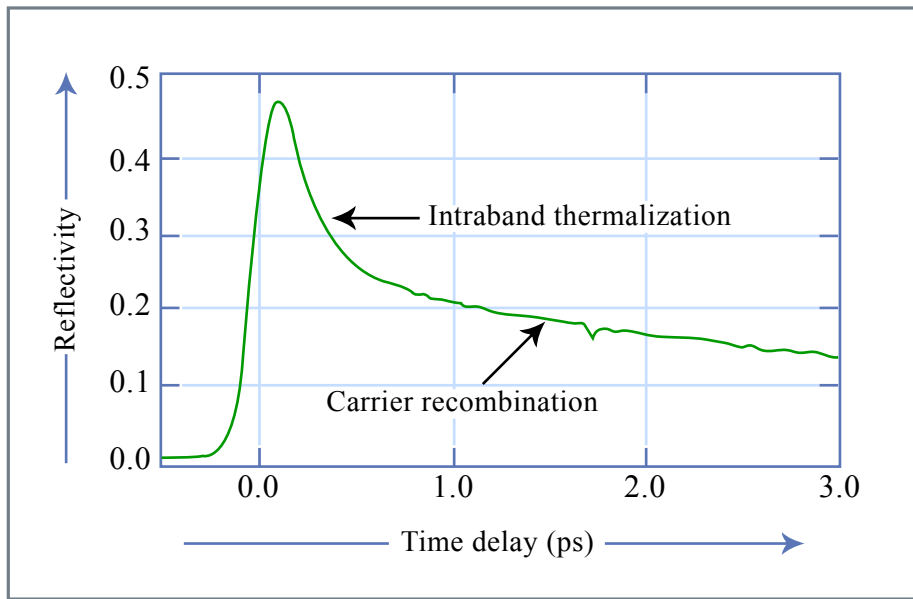


Figure 8.5: Pump probe response of a semiconductor saturable absorber mirror with a multiple-quantum well InGaAs saturable absorber grown at low temperature [3].

Figure by MIT OCW.

With the formula for the saturation intensity of a two-level system Eq. (2.145), we can estimate a typical value for the saturation fluence $F_s$ (saturation energy density) of a semiconductor absorber for interband transitions. The saturation fluence $F_A$, also related to the absorption cross-section $\sigma_A$, is

then given by

$$F_A \;\; = \;\; \frac{hf}{\sigma_A} = I_A \tau_A = \frac{\hbar^2}{2T_2 Z_F \left| \vec{M} \right|^2} \tag{8.1}$$

$$= \;\; \frac{\hbar^2 n_0}{2T_2 Z_{F0} \left| \vec{M} \right|^2} \tag{8.2}$$

The value for the dipole moment for interband transitions in III-V semiconductors is about $d = 0.5$ nm with little variation for the different materials. Together with the a dephasing time on the order of $T_2 = 20$ fs and a linear refractive index $n_0 = 3$, we obtain

$$F_A = \frac{\hbar^2 n_0}{2T_2 Z_{F0} \left| \vec{M} \right|^2} = 35 \frac{\mu J}{cm^2} \tag{8.3}$$

Figure 8.6 shows the saturation fluence measurement and pump probe trace with 10 fs excitation pulses at 800 nm on a broadband GaAs semiconductor saturable absorber based on a metal mirror shown in Figure 8.7 [11]. The pump probe trace shows a 50 fs thermalization time and long time bleaching of the absorption recovering on a 50 ps time scale due to trapping and recombination.

Image removed due to copyright restrictions.

Please see:

Jung, I. D., et al. "Semiconductor saturable absorber mirrors supporting sub-10 fs pulses."
*Applied Physics B* 65 (1997): 137-150.

Figure 8.6: Saturation fluence and pump probe measurements with 10 fs pulses on a broadband metal mirror based GaAs saturable absorber. The dots are measured values and the solid line is the fit to a two-level saturation characteristic [11].

A typical value for the fluence at wich damage is observed on an absorber is on the order of a few mJ/cm$^2$. Saturating an absorber by a factor of 10 without damaging it is still possible . The damage threshold is strongly dependent on the growth, design, fabrication and mounting (heat sinking) of the absorber.

Image removed due to copyright restrictions.

Please see:

Fluck, R., et al. "Broadband saturable absorber for 10 fs pulse generation." *Optics Letters* 21 (1996): 743-745.

Figure 8.7: GaAs saturable absorber grown an GaAs wafer and transfered onto a metal mirror by post growth processing [10].

## 8.2 High Fluence Effects

To avoid Q-switched mode-locking caused by a semiconductor saturable absorber, the absorber very often is operated far above the saturation fluence or enters this regime during Q-switched operation. Therefore it is also important to understand the nonlinear optical processes occuring at high excitation levels [13]. Figure 8.8 shows differential pump probe measurements on a semiconductor saturable absorber mirror similar to Figure 8.2 but adapted to the 1.55 $\mu m$ range for the developement of pulsed laser sources for optical

communication. The structure is a GaAs/AlAs-Bragg-mirror with an InP half-wave layer and an embedded InGaAsP quantum well absorber with a band edge at 1.530 $\mu m$. The mirror is matched to air with an $Al_2O_3$ single-layer Ar-coating. At low fluence (5.6 $\mu J$) the bleaching dynamics of the QWs are dominant. At higher fluences, two-photon absorption (TPA) and free carrier absorption (FCA) in the InP half-wave layer develop and enventually dominate [13].
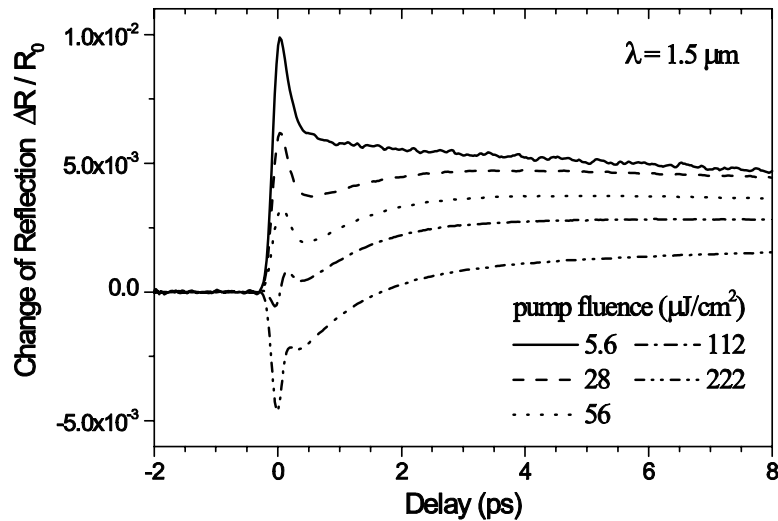


Figure 8.8: Differential reflectivity measurements of a semiconductor saturable absorber mirror (GaAs/AlAs-Bragg-mirror and InP half-wave layer with embedded InGaAsP quantum well absorber for the 1.55 $\mu m$ range. The mirror is matched to air with an $Al_2O_3$single-layer ar-coating). At low fluence the bleaching dynamics of the QWs are dominant. At higher fluences, TPA and FCA develop and enventually dominate [13].

The assumption that TPA and FCA are responsible for this behaviour has been verified experimentally. Figure 8.9 shows differential reflectivity measurements under high fluence excitation at 1.56 $\mu m$ for a saturable absorber mirror structure in which absorption bleaching is negligible (solid curve). The quantum well was placed close to a null of the field. A strong TPA peak is followed by induced FCA with a single $\sim$ 5ps decay for FCA. Both of these dynamics do not significantly depend on the wavelength of the excitation, as long as the excitation remains below the band gap. The $\sim$ 5ps decay is

attributed to carrier diffusion across the InP half-wave layer [13] The dashed curve shows the differential absorption of a $\sim 350 \; \mu m$ thick InP substrate in which a standing-wave pattern is not formed and the $\sim$ 5ps decay is absent. The inset in Figure 8.9 shows the power dependence of TPA and FCA. As expected, TPA and FCA vary linearly and quadratically, respectively, with pump power.The pump-induced absorption of the probe (TPA) is linearly dependent on the pump power. Since FCA is produced by carriers that are generated by the pump alone via TPA, FCA scales with the square of the pump power.
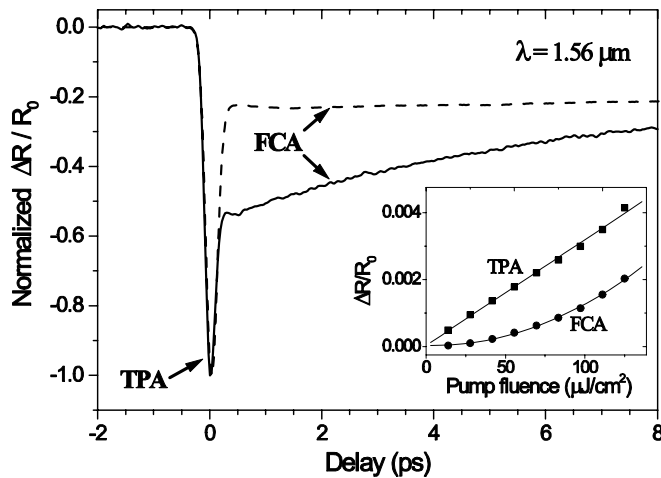


Figure 8.9: Differential reflectivity measurements under high fluence excitation at 1.56 $\mu m$ for a saturable absorber mirror structure in which absorption bleaching is negligible (solid cuve). The $\sim$ 5 ps decay for FCA is attributed to carrier diffusion across the InP half-wave layer. The dahed curve shows the differential absorption of a $\sim 350 \; \mu m$ thick InP substrate in which a standing-wave pattern is not formed. (Inset) Linear and quadratic fluence dependence of the TPA and FCA components, respectively.

These high fluence effects lead to strong modifications of the saturation characteristics of a saturable absorber. The importance of the high fluence effects was first recognized in resonant absorbers (see Figure 8.10). The field inside the absorber is enhanced by adding a top reflector and a proper spacer layer. This leads to an effective lower saturation fluence when viewed with

respect to the intracavity fluence or intensity. Therefore, high fluenece effects are already reached at low intracavity intensities (see Figure 8.9).
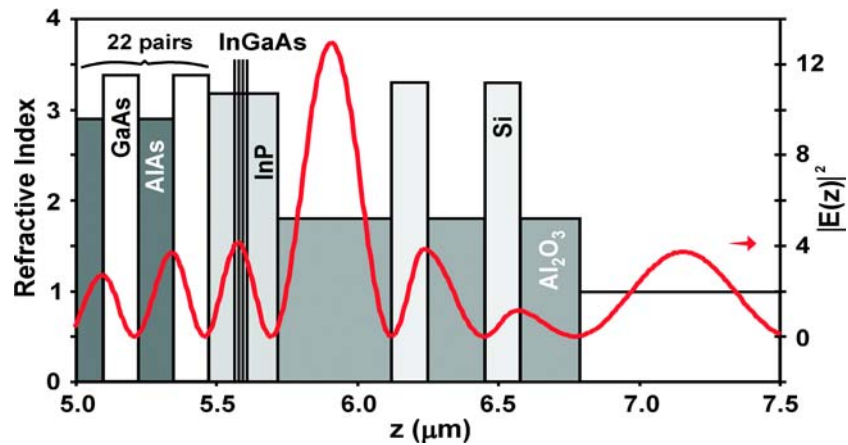


Figure 8.10: A top reflector is added to the semiconductor saturable absorber such that the field in the quantum well is resonantely enhanced by about a factor of 10 in comparison to the non resonant case.

Figure 8.11: Saturation fluence measurement (dots) of the resonant absorber shown in Figure 8.10 with 150 fs pulses at 1.53 $\mu m$. Fits are shown using a fast or slow saturable absorber and TPA. Also the scaled saturation characteristics of the absorber are shown when used in a laser with longer pulse durations.

Theon, E. R., et al. "Two-photon absorption in semiconductor saturable absorber mirrors." *Applied Physics Letters* 74 (1999): 3927-3929. Used with permission.
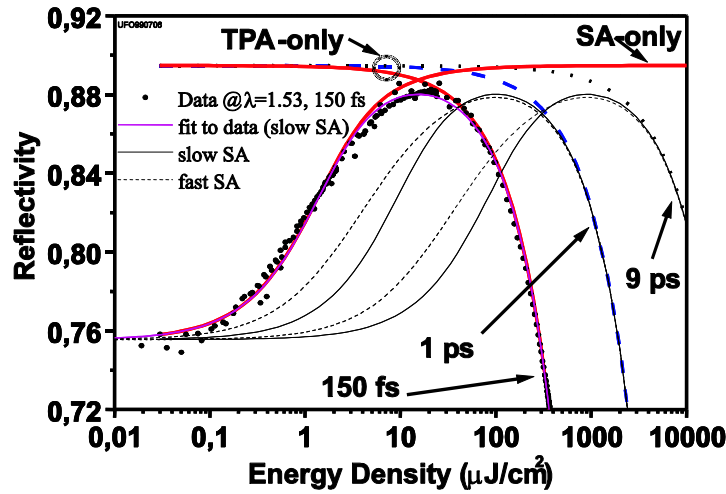
The roll-over of the saturation characteristics has positive and negative consequences for mode locking. First, if the roll-over can be reached with the available intracavity pulse energy, Q-switching can be suppressed. Second if the roll-over occurs too early, the pulses break up into multiple pulses to optimize the net gain for the overall pulse stream.

## 8.3    Break-up into Multiple Pulses

In the treatment of mode locking with fast and slow saturable absorbers we only concentrated on stability against energy fluctuations (Q-switched mode locking) and against break through of cw-radiation or continuum. Another often observed instability is the break-up into multiple pulses. The existence of such a  mechanism is obvious if soliton pulse shaping processes are present. If we assume that the pulse is completely shaped by the solitonlike pulse shaping processes, the FWHM pulse width is given by

$$\tau_{FWHM} = 1.76 \frac{4\,|D_2|}{\delta W}. \tag{8.4}$$

where $W$ denotes the pulse energy. $D_2$ the negative disperison and $\delta$ the self-phase modulation coefficient. With increasing pulse energy, of course the absorber becomes more strongly saturated, which leads to shorter pulses according to the saturable absorber and the soliton formula. At a certain point, the absorber will saturate and can not provide any further pulse stabilization. However, the Kerr nonlinearity may not yet saturate and, therefore, the soliton formula dictates an ever decreasing pulse width for increasing pulse energy. Such a process continues, until either the continuum breaks through, because the soliton loss becomes larger than the continuum loss, or the pulse breaks up into two pulses. The pulses will have reduced energy per pulse and each one will be longer and experiences a reduced loss due to the finite gain bandwidth. Due to the reduced pulse energy, each of the pulses will suffer increased losses in the absorber, since it is not any longer as strongly saturated as before. However, once the absorber is already over saturated by the single pulse solution, it will also be strongly saturated for the double-pulse solution. The filter loss due to the finite gain bandwidth is heavily reduced for the double-pulse solution. As a result, the pulse will break up into double-pulses. To find the transition point where the break-up into multiple pulses occurs, we write down the round-trip loss due to the gain and filter losses and the saturable absorber according to 6.35

$$l_m = \frac{D_f}{3\tau_m^2} + q_s(W_m), \tag{8.5}$$

where, $q_s(W_m)$ is the saturation loss experienced by the pulse when it propagates through the saturable absorber. This saturation loss is given by

$$q_s(W) = \frac{1}{W} \int\limits_{-\infty}^{+\infty} q(T,t)|A_s(t)|^2 dt. \tag{8.6}$$

This expression can be easily evaluated for the case of a sech-shaped steady state pulse in the fast saturable absorber model with

$$q_{fast}(t) = \frac{q_0}{1 + \frac{|A(t)|^2}{P_A}}, \quad \text{where} \quad P_A = \frac{E_A}{\tau_A}. \tag{8.7}$$

and the slow saturable absorber model, where the relaxation term can be neglected because of $\tau_A \gg \tau$.

$$q_{slow}(t) = q_0 \exp\left[-\frac{1}{E_A}\int_{-\infty}^{t}|A_s(t')|^2 dt'\right]. \tag{8.8}$$

For the slow absorber 8.8 the absorber losses (8.6) can be evaluated indepen-
dent of pulse shape to be

$$q_{s.slow}(W) = q_0 \frac{1 - \exp\left[-\frac{W}{E_A}\right]}{\frac{W}{E_A}}. \tag{8.9}$$

Thus for a slow absorber the losses depend only on pulse energy. In contrast,
for a fast absorber, the pulse shape must be taken into account and, for a
sech-shaped pulse, one obtaines [14]

$$q_{s,fast}(W) = q_0 \sqrt{\frac{1}{\alpha(1+\alpha)}} \tanh^{-1}\left[\sqrt{\frac{\alpha}{1+\alpha}}\right], \text{ with } \alpha = \frac{W}{2P_A\tau}, \tag{8.10}$$

and the pulse energy of one pulse of the multiple pulse solution. The energy
is determined from the total gain loss balance

$$\frac{g_0}{1 + \frac{mW_m}{P_L T_R}} = l + l_m. \tag{8.11}$$

Most often, the saturable absorber losses are much smaller than the losses
due to the output coupler. In that case the total losses are fixed independent
of the absorber saturation and the filter losses. Then the average power does
not depend on the number of pulses in the cavity. If this is the case, one
pulse of the double pulse solution has about half of the energy of the single
pulse solution, and, therefore, the width of the double pulse is twice as large
as that of the single pulse according to (8.4). Then the filter and absorber
losses for the single and double pulse solution are given by

$$l_1 = \frac{D_f}{3\tau_1^2} + q_s(W_1), \tag{8.12}$$

$$l_2 = \frac{D_f}{12\tau_1^2} + q_s(\frac{W_1}{2}). \tag{8.13}$$

The single pulse solution is stable against break-up into double pulses as long
as

$$l_1 \leq l_2 \tag{8.14}$$

is fulfilled. This is the case, if the difference in the filter losses between the
single and double pulse solution is smaller than the difference in the saturable
absorber losses

$$\frac{D_f}{4\tau_1^2} < \Delta q_s(W) = q_s(\frac{W}{2}) - q_s(W). \tag{8.15}$$

Figure 8.12 shows the difference in the saturable absorption for a single pulse and a double pulse solution as a function of the ratio between the single pulse peak power and saturation power for a fast absorber and as a function of the ratio between the single pulse energy and saturation energy for a slow absorber. Thus, for both cases the optimum saturation ratio, at which the largest discrimination between single and double pulses occurs and, therefore, the shortest pulse before break-up into multiple pulses occurs, is about 3. Note, that to arrive at this absolute number, we assumed that the amount of saturable absoption is neglegible in comparison with the other intracavity losses, so that the saturated gain level and the gain and filter dispersion are fixed.

Image removed due to copyright restrictions.

Please see:

Kartner, F. X., J. A. d. Au, and U. Keller. "Mode-Locking with Slow and Fast Saturable Absorbers-- What's the Difference." *Selected Topics in Quantum Electronics* 4 (1998): 159.

Figure 8.12: Difference in loss experienced by a sech-shaped pulse in a slow (- - -) and a fast (_ _ _ _) saturable absorber for a given pulse energy or peak power , respectively.

At this optimum operation point, the discrimination against multiple break-up of a fast absorber is about 50% larger than the value of the slow absorber. Since the minimum pulsewidth scales with the square root of $\Delta q_s(W)$, see Eq. (8.15), the minimum pulsewidth of the slow absorber is only about 22% longer than with an equally strong fast saturable absorber. Figure 8.12 also predicts that a laser modelocked by a fast saturable absorber is much more stable against multiple pulse break-up than a slow saturable absorber if it is oversaturated . This is due to the fact that a fast saturable absorber saturates with the peak power of the pulse in comparison with a slow saturable absorber, which saturates with the pulse energy. When the pulse breaks up into a pulse twice as long with half energy in each, the peak power of the

individual pulses changes by a factor of four. Therefore, the discrimination between long and short pulses is larger in the case of a fast saturable absorber, especially for strong saturation. Note that Fig. 8.12 is based on the simple saturation formulas for fast and slow saturable absorbers Eqs. (8.9) and (8.10). We compare these predictions with numerical simulations and experimental observations made wiht a Nd:glass laser [15][16].

The Nd:glass laser described in ref. [15] was modelocked by a saturable absorber which showed a fast recovery time of $\tau_A = 200$ fs, a modulation depth of $q_0 = 0.005$ and a saturation energy of $E_A = 17$ $nJ$. The other laser parameters can be found in [16]. Without the solitonlike pulse formation (GDD and SPM is switched off), the laser is predicted to produce about 200 fs short pulses with a single pulse per round-trip, very similar to what was discussed in the fast saturable absorber mode locking in Chapter 6. The dynamics becomes very much different if the negative GDD and positive SPM are included in the simulation, (see Figure 8.13)

Image removed due to copyright restrictions.

Please see:

Kartner, F. X., J. A. d. Au, and U. Keller. "Mode-Locking with Slow and Fast Saturable Absorbers-- What's the Difference." *Selected Topics in Quantum Electronics* 4 (1998): 159.

Figure 8.13: Each trace shows the pulse intensity profile obtained after 20,000 cavity round-trips in a diode-pumped Nd:glass laser according to [15]. When the laser reaches the double-pulse regime the multipel pulses are in constant motion with respect to each other. The resulting pulse train is not any longer stationary in any sense.

With increasing small signal gain, i. e. increasing pulse energy, the soliton shortens to 80 fs due to the solitonlike pulse shaping, (Figure 8.13).

Image removed due to copyright restrictions.

Please see:

Kartner, F. X., J. A. d. Au, and U. Keller. "Mode-Locking with Slow and Fast Saturable Absorbers-- What's the Difference." *Selected Topics in Quantum Electronics* 4 (1998): 159.

Figure 8.14: Steady state pulse width ($\circledR$) and time-bandwidth product (o) for a Nd:glass laser modelocked by a saturable absorber with a 200 fs recovery time with GDD and SPM included, shown as a function of the intracavity pulse energy. The time-bandwidth product is only meaningful in the single pulse regime, where it is shown. The pulses are almost transform limited sech-pulses. The pulse width in the multiple pulseing regime is only unique in the parameter region where multiple pulses of similar height and width are achieved. The pulses break up into multiple pulses when the absorber is about three times saturated.

The pulse width follows nicely the soliton relation (8.4), (dash-dotted line). The pulses become shorter, by about a factor of 2.5, than without GDD and SPM before the pulse breaks up into longer double-pulses. The pulse break-up into double-pulses occurs when the absorber is about two times saturated, close to the point where the shortest pulse can be expected according to the discussion above. Figures 8.13 shows, that the break-up point for the double pulses is also very close to the instability for continuum break-through. Indeed the first pulse train after break-up at a small signal gain of $g_0 = 0.09$ shows the coexistance of a longer and a shorter pulse, which indicates continuum break-through. But the following five traces are double pulses of equal height and energy. For even stronger saturation of the

absorber the double-pulses break-up into triple pulses and so on. Then the dynamics becomes even more complex. This behavior has been observed in detail in a Nd:glass laser [15], (see Figure 8.15), as well as in Cr4+:YAG lasers [17]. The simulations just discussed match the parameters of the Nd:glass experiments.

Figure 8.15: Pulsewidth in a Nd:glass laser [15] as a function of intracavity stored energy, i.e. pulse energy for a single pulse per round-trip. Dots measured values and solid line fits for a single and double-pulse solitonlike pulse stream.

Figure 8.15 clearly shows the scaling of the observed pulse width according to the soliton formula until the pulses break up at a saturation ratio of about 2. Notice, that the absorber recovery time of 200 fs is not much shorter than the pulse width achieved. Nevertheless, the optimum saturation ratio is close to the expected one of about 3. The break-up into pure double and triple pulses can be observed more clearly if the absorber recovery time is chosen to be shorter, so that continuum break-through is avoided. Figure 8.16 shows the final simulation results obtained after 20,000 round-trips in the cavity, if we reduce the absorber recovery time from 200 fs to 100 fs, again for different small signal gain, e.g. intracavity power levels and pulse energies. Now, we observe a clean break-up of the single-pulse solution into double-pulses and at even higher intracavity power levels the break-up into triple pulses without continuum generation in between. Note that the spacing between the pulses is very much different from what has been observed for the 200 fs response time. This spacing will depend on the details of the absorber and may also

be influenced by the dynamic gain saturation even if it is only a very small effect in this case [17].

Image removed due to copyright restrictions.

Please see:

Kartner, F. X., J. A. d. Au, and U. Keller. "Mode-Locking with Slow and Fast Saturable Absorbers--What's the Difference." *Selected Topics in Quantum Electronics* 4 (1998): 159.

Figure 8.16: Each trace shows the pulse intensity profile obtained after 20,000 cavity round-trips for an absorber with a response time $\tau_A = 100$ fs for different values of the small-signal gain. The simulations are always started with a 1 ps initial pulse shown as the first trace. Note that only the single pulse solutions are stationary.

## 8.4   Summary

Real absorbers do have the advantage of providing direct amplitude modulation and do not exploit additional cavities or operation of the resonator close to its stability boundary to achieve effective phase to amplitude conversion. Especially in compact resonator designs, as necessary for high-repitition rate lasers in the GHz range, semiconductor saturable absorbers with their low saturation energies and compactness offer unique solutions to this important technological challenge.

# Bibliography

[1] M. N. Islam, E. R. Sunderman, C. E. Soccolich, I. Bar-Joseph, N. Sauer, T. Y. Chang, and B. I. Miller: "Color Center Lasers Passively Mode Locked by Quantum Wells," IEEE J. Quantum Electronics. **25**, 2454-2463 (1989).

[2] S. Tsuda, W. H. Knox, E. A. de Souza, W. Y. Jan, and J. E. Cunningham, "Mode-Locking Ultrafast Solid-State Lasers with Saturable-Bragg Reflectors," IEEE J. Sel. Top. Quantum Electronics **2**, 454-464 (1996).

[3] U. Keller, "Semiconductor nonlinearities for solid-state laser modelocking and Q-switching," in Semiconductors and Semimetals, Vol. **59**A, edited by A. Kost and E. Garmire, Academic Press, Boston 1999.

[4] J. Shah, "Ultrafast Spectroscopy of Semiconductors and Semiconductor Nanostructures," Series in Solid-State Sciencies **115**, Springer Verlag, Berlin (1996).\

[5] E. O. Goebel, "Ultrafast Spectroscopy of Semiconductors," in Advances in Solid State Physics **30**, pp. 269 – 294 (1990).

[6] W. H. Knox, R. L. Fork, M. C. Downer, D. A. B. Miller, D. S. Chemla and C. V. Shank, "Femtosecond Excitation of Nonthermal Carrier Populations in GaAs Quantum Wells," Phys. Rev. Lett. **54**, pp. 1306 – 1309 (1985).

[7] J. L. Oudar, D. Hulin, A. Migus, A. Antonetti, F. Alexandre, "Subpicosecond Spectral Hole Burning Due to Nonthermalized Photoexcited Carriers in GaAs," Phys. Rev. Lett. **55**, pp. 2074 – 2076 (1985).

[8] W. H. Knox, C. Hirlimann, D. A. B. Miller, J. Shah, D. S. Chemla and C. V. Shank, "Femtosecond Dynamics of Resonantly Excited Excitons in

Room-Temperature GaAs Quantum Wells," Phys. Rev. Lett. **56**, 1191 – 1193 (1986).

[9] G. L. Witt, R. Calawa, U. Mishra, E. Weber, Eds., "Low Temperature (LT) GaAs and Related Materials," **241,** Pittsburgh, (1992).

[10] R. Fluck, I. D. Jung, G. Zhang, F. X. Kärtner, and U. Keller, "Broadband saturable absorber for 10 fs pulse generation," Opt. Lett. **21**, 743-745 (1996).

[11] I. D. Jung, F. X. Kärtner, N. Matuschek, D. H. Sutter, F. Morier-Genoud, Z. Shi, V. Scheuer, M. Tilsch, T. Tschudi, U. Keller, "Semiconductor saturable absorber mirrors supporting sub-10 fs pulses," Appl. Phys. B **65**, pp. 137-150 (1997).

[12] E. R. Thoen, E. M. Koontz, M. Joschko, P. Langlois, T. R. Schibli, F. X. Kärtner, E. P. Ippen, and L. A. Kolodziejski, "Two-photon absorption in semiconductor saturable absorber mirrors," Appl. Phys. Lett. 74, 3927-3929, (1999).

[13] P. Langlois, M. Joschko, E. R. Thoen, E. M. Koontz, F. X. Kärtner, E. P. Ippen, and L. A. Kolodziejski, "High fluence ultrafast dynamics of semiconductor saturable absorber mirrors," Appl. Phys. Lett. 75, 3841-3483, (1999).

[14] T. R. Schibli, E. R. Thoen, F. X. Kaertner, E. P. Ippen, "Suppression of Q-switched mode-locking and break-up into multiple pulses by inverse saturable absorption," App. Phys. B **70**, 41-49 (2000).

[15] J. Aus der Au, D. Kopf, F. Morier-Genoud, M. Moser and U. Keller, "60-fs pulses from a diode-pumped Nd:glass laser," Opt. Lett. **22**, 207-309 (1997).

[16] F.X. Kärtner, J. A. d. Au, U. Keller, "Mode-Locking with Slow and Fast Saturable Absorbers-What's the Difference,". Sel. Top. Quantum Electron. **4**, 159 (1998).

[17] B. C. Collings, K. Bergman, W. H. Knox, "Truely fundamental solitons in a passively mode-locked short cavity Cr4+:YAG laser.," Opt. Lett., **22**,1098-1100 (1997).